Local impurity effects in superconducting graphene

T. O. Wehling,[1] H. P. Dahal,[2] A. I. Lichtenstein,[1] and A. V. Balatsky[2,3,*]
[1]*Institut für Theoretische Physik, Universität Hamburg, Jungiusstraße 9, D-20355 Hamburg, Germany*
[2]*Theoretical Division, Los Alamos National Laboratory, Los Alamos, New Mexico 87545, USA*
[3]*Center for Integrated Nanotechnologies, Los Alamos National Laboratory, Los Alamos, New Mexico 87545, USA*
(Received 6 June 2008; published 9 July 2008)

We study the local electronic properties of superconducting graphene in presence of impurities. In particular, we consider the case of magnetic and nonmagnetic impurities being either strongly localized or acting as a potential averaged over one unit cell. The spin dependent local density of states (LDOS) is calculated and possibilities for identifying the superconducting order parameter in graphene by means of scanning tunneling experiments are pointed out. We show that the vanishing effective mass of the electrons results in no coherence peaks at the superconducting gap edge. A method for identifying magnetic scatterers even by non-spin-polarized scanning tunneling spectroscopy is given.

DOI: 10.1103/PhysRevB.78.035414 PACS number(s): 74.45.+c, 68.37.Ef, 71.55.−i

I. INTRODUCTION

Graphene—a monolayer of carbon atoms arranged in a honeycomb lattice—is one of the most promising materials for postsilicon electronics[1] and thanks to its electronic structure graphene provides a model system for studying relativistic quantum physics in condensed matter.[2,3] Being the basis of many electronic devices, impurity states are important for technological applications but allow one here to also address fundamental questions of relativistic scattering.[4–8] It turned out that impurities can change clean graphene's linearly vanishing density of states (DOS) substantially. Strong impurities cause virtual bound states (VBS), i.e., resonances in the DOS, which may be arbitrarily sharp in the vicinity of the Dirac point. The broad similarities of these impurity states with states in *d*-wave superconductors have been used to discuss common aspects of impurity scattering in superconductors and in graphene.[5,6,8–10]

Recently, proximity induced superconductivity in graphene has been demonstrated[11] and has opened exciting opportunities for experiments: Superconducting graphene is an explicit example of valleytronics,[12] where opposite valleys are nontrivially coupled. A prior analysis of ballistic superconducting transport[13] revealed an interesting suppression of the critical current near the Dirac point. However, the response of the superconducting state to impurities, which is directly related to the symmetry of the order parameter, is still unknown. In particular, the possibility of intragap bound states and the impact of gap opening on the Friedel oscillations in the continuum are open questions that must be answered to understand the stability of the superconducting state in graphene and to extract the symmetry of the order parameter from local spectroscopy:[9] According to the Anderson theorem,[14] nonmagnetic impurities will be able to produce impurity resonances inside the superconducting gap for all symmetries of the order parameter except for *s*-wave pairing. It is therefore a fingerprint of *s*-wave superconductivity, if nonmagnetic impurities do not cause intragap resonances in scanning tunneling spectra.[15]

In this paper, we theoretically investigate proximity induced superconductivity in graphene and study impurity effects on the local density of states. In the proximity effect, the pairing state of the Cooper pairs tunneling from the superconductor to graphene, will be controlled by the pairing state of the superconductor. As in the case of the experiment by Heersche *et al.*,[11] we consider *s*-wave Cooper pairs in graphene. The Hamiltonian describing this scenario is explained in Sec. II and, in Sec. III, it is used to calculate the local density of states (LDOS) of superconducting graphene with and without impurities. For clean superconducting graphene, we find no coherence peaks at the gap edge, which is in contrast to other superconductors like Nb. Near magnetic impurities, bound states *inside* the superconducting gap are found to occur. These bound states *always* coexist with the formerly studied VBS in the continuum.[8] Thus, the predicted impurity states are similar to the magnetic impurity induced Yu Lu-Shiba-Rusinov states in usual *s*-wave superconductors.[9,15] Due to its two-dimensionality graphene is well suited for scanning tunneling microscopy (STM) and STM on normal-state graphene already indicates the importance of impurity effects in this context.[16,17] It is therefore simply a matter of time (see e.g., Ref. 18) before impurity states in superconducting graphene are addressed locally. In Sec. IV, we elucidate the real-space shape of these impurity states, which will be directly observable in STM.

While intrinsic superconductivity in graphene is controversial,[19] Ti/Al bilayer contacts placed on the graphene sheet induce a measured supercurrent.[11] No spectral gap in the samples has been measured to date. We argue that any type of electron-electron interaction in the graphene will produce a gap in the spectrum when Cooper pairs are *injected*. This gap Δ will be proportional to the interaction strength and it remains to be seen how large it can be in graphene. Electron spectroscopy such as STM and/or planar tunneling into graphene in proximity to superconducting leads would be able to reveal this spectroscopic gap. We will treat Δ below as a phenomenological parameter that needs to be determined separately. Furthermore, we describe graphene in this proximity regime using Bogoliubov–de Gennes theory, since screening is rather efficient in this material.[20]

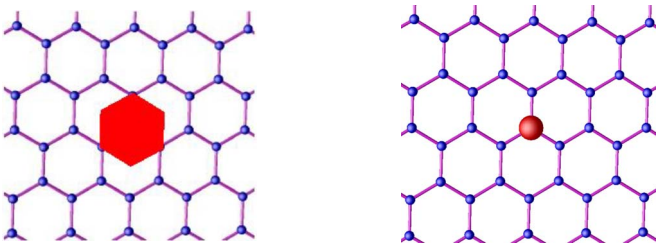

FIG. 1. (Color online) Among the various local impurities we discuss two limiting cases. The scalar impurity (left), V_s, corresponds to a uniform potential averaged over one unit cell, whereas the on-site impurity (right), V_o, acts on one sublattice only.

II. MODEL OF IMPURITIES IN SUPERCONDUCTING GRAPHENE

Low energy electronic excitations in graphene can be described by two species of Dirac fermions located around two nodal points $K^{\pm}$ in the Brillouin zone with the speed of light being replaced by the Fermi velocity v_f and the corresponding Hamiltonian $H_{K^{\pm}}=v_f\hbar(k_1\sigma_1 \mp k_2\sigma_2)$. σ_i, $i=1,2,3$, are Pauli matrices acting on the sublattice degrees of freedom and σ_0 is the identity matrix. To understand impurities in superconducting graphene, we rewrite the above Hamiltonian to the Nambu formalism including both valleys:

$$\hat{H} = -i\hbar v_f \int \mathrm{d}^2x \hat{\Psi}^{\dagger}(x)(\partial_1\sigma_1 \otimes \tau_0 - \partial_2\sigma_2 \otimes \tau_3) \otimes \Lambda_0 \hat{\Psi}(x),$$

with $\hat{\Psi}(x)^{\dagger}=[\Psi^{\dagger}_{\downarrow K^+}(x),\Psi^{\dagger}_{\downarrow K^-}(x),\Psi_{\uparrow K^-}(x),\Psi_{\uparrow K^+}(x)]$ and $\Psi_{\uparrow\downarrow K^{\pm}}(x)$ being field operators of electrons with a spin $\uparrow\downarrow$ and belonging to a valley $K^{\pm}$. τ_i and Λ_i with $i=1,2,3$ are Pauli matrices acting on the valley and Nambu space, respectively. τ_0 and Λ_0 are the corresponding identity matrices. In this formalism the proximity induced pairing potential enters as $\Delta\sigma_3\otimes\tau_0\otimes\Lambda_1$ and results in electron dynamics being described by the Dirac–Bogoliubov–de Gennes Hamiltonian:[21]

$$H = -i\hbar v_f(\partial_1\sigma_1 \otimes \tau_0 - \partial_2\sigma_2 \otimes \tau_3) \otimes \Lambda_0 + \Delta\sigma_3 \otimes \tau_0 \otimes \Lambda_1. \tag{1}$$

To elucidate the effect of different impurities (see Fig. 1), we discuss both a homogeneous potential acting within one unit cell V_s ("scalar impurity") as well as a strongly localized impurity V_o ("on-site impurity") acting only at sublattice A and giving rise to intervalley scattering. Starting from impurity operators in the tight-binding form of, e.g., Ref. 8, and using the conventions of Eq. (1) we obtain the following explicit expressions for the impurity potentials in the adopted matrix notation: $V_s=V_0\sigma_0\otimes\tau_0\otimes\Lambda_3+V_1\sigma_0\otimes\tau_0\otimes\Lambda_0$ and $V_o=V_0(\sigma_3+\sigma_0)\otimes(\tau_0+\tau_1)\otimes\Lambda_3+V_1(\sigma_3+\sigma_0)\otimes(\tau_0+\tau_1)\otimes\Lambda_0$. In both cases V_0 and V_1 describe the electrostatic and magnetic contribution to the impurity potential, respectively.

III. IMPURITY RESONANCES

The effect of these impurities on the local electronic properties of the superconducting graphene sheets is contained in the LDOS, which we calculate using the T-matrix approach:[9] In operator form, the full Green's function $G(\omega)$ in presence of the impurity is obtained from the unperturbed Green's function $G^0(\omega)$ via $G(\omega)=G^0(\omega)+G^0(\omega)T(\omega)G^0(\omega)$ with $T(\omega)=V_{s(o)}(1-G^0(\omega)V_{s(o)})^{-1}$. Dealing with local impurities, it is convenient to adopt the position space representation. Therefore, the free x-dependent Green's function $\hat{G}^0(x,\omega)$ in polar coordinates, $x=x(r,\phi)$, is obtained from its momentum space counterpart $\hat{G}^0(p,\omega)=(\omega-H)^{-1}$ by Fourier transformation

$$\begin{aligned}\hat{G}^0(x,\omega) &= \int \frac{\mathrm{d}^2p}{\Omega_B}\hat{G}^0(p,\omega)e^{ipx} \\ &= g_0(r,\omega)(\omega\sigma_0 \otimes \tau_0 \otimes \Lambda_0 + \Delta\sigma_3 \otimes \tau_0 \otimes \Lambda_1) \\ &\quad + g_1(r,\omega)\{[\cos\phi\sigma_1 \otimes \tau_0 + \sin\phi\sigma_2 \otimes \tau_3] \otimes \Lambda_0\},\end{aligned} \tag{2}$$

with $g_0(r,\omega)=v_f^2\int_0^{p_c}\mathrm{d}pppJ_0(pr)[W^2(\omega^2-\Delta^2-v_f^2p^2)]^{-1}$ and $g_1(r,\omega)=iv_f^3\int_0^{p_c}\mathrm{d}pp^2J_1(pr)[W^2(\omega^2-\Delta^2-v_f^2p^2)]^{-1}$, where we expressed the Brillouin zone volume $\Omega_B=2\pi W^2/v_f^2$ in terms of the bandwidth W. The Green's function at $x=0$ determines the LDOS of the clean system: $\hat{G}^0(0,\omega+i\delta)=M(\omega)(\omega\sigma_0\otimes\tau_0\otimes\Lambda_0+\Delta\sigma_3\otimes\tau_0\otimes\Lambda_1)$. Here $M(\omega)=M'(\omega)+iM''(\omega)$ with $M'(\omega)=\frac{1}{2W^2}\ln\left|\frac{\Delta^2-\omega^2}{W^2+\Delta^2-\omega^2}\right|$ and $M''(\omega)=-\frac{\pi\,\mathrm{sgn}(\omega)}{2W^2}$ for $\Delta^2<\omega^2<\Delta^2+W^2$ and $M''(\omega)=0$ otherwise. The corresponding LDOS vanishes within the superconducting gap ($\omega^2<\Delta^2$) and is given by $N_0(\omega)=\frac{4|\omega|}{W^2}$ outside the gap, which is quite different from usual BCS superconductors as there are *no* coherence peaks at the gap edge.

In general, impurity resonances occur when the T matrix becomes (almost) singular, i.e., $\det(1-G^0(0,\omega)V)=0$. For the scalar impurity this secular equation yields $1-2M(\omega)\omega V_1+M^2(\omega)(\omega^2-\Delta^2)(V_1^2-V_0^2)=0$ with solutions that can be understood analytically in the following limiting cases: First consider a solely magnetic impurity, i.e., $V_0=0$, with $V_1>0$. In the Born limit the solutions $\omega_0=-\Delta\pm\delta\omega$ with

$$\delta\omega = \frac{W^2}{2\Delta}e^{-W^2/(\Delta V_1)} \tag{3}$$

give rise to intragap bound and virtual bound states in the continuum approaching the gap edge exponentially with decreasing V_1. In the opposite limit of unitary scattering $\omega_0=\pm\Delta-\delta\omega$ with

$$\delta\omega = -\frac{2W^2}{V_1\ln\left(\frac{2\Delta}{V_1}\right)} \tag{4}$$

fulfills the secular equation, where the upper (lower) sign corresponds to an intragap bound (continuum virtual bound) state.

The numerical solutions to energies of the intragap bound states are shown in Fig. 2. It recovers the limiting cases obtained analytically and demonstrates also the effect of an electrostatic contribution V_0 to the impurity potential: In the Born limit, the exponential dependence of $\delta\omega$ on the magnetic potential strength V_1 is dominant and suppresses any significant influence of V_0 on the impurity state energy. In the

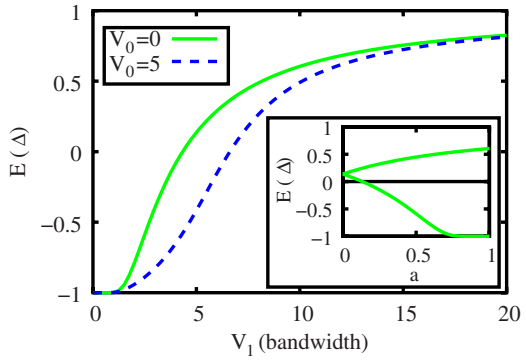

FIG. 2. (Color online) Energy of the impurity resonance for the scalar impurity as a function of the magnetic impurity potential V_1 for different electrostatic potentials V_0. The gap-parameter is $\Delta = W/10$. The lower right inset shows the splitting of the impurity state due to intervalley scattering. We model intervalley scattering as $V = V_1(\sigma_0 \otimes \tau_0 \otimes \Lambda_0 + a\sigma_0 \otimes \tau_1 \otimes \Lambda_0)$ with the strength of the intervalley scattering parametrized by a and $V_1 = 5$ W. One split state is shifted to the gap edge; the other state remains an intragap state.

$V_1 \to \infty$ limit, V_0 leads to a renormalization of the *effective* magnetic potential strength $V_1 \to V_1(1 - \frac{V_0^2}{V_1^2})$. As Fig. 2 shows, the effect of an additional electrostatic potential becomes most pronounced in the intermediate region. There, the electrostatic contribution reduces the effective magnetic potential strength most significantly.

To elucidate the effect of intervalley scattering, we compare the strongly localized on-site impurities with the scalar impurities discussed above. Due to valley degeneracy, the scalar impurity gives rise to doubly degenerate intragap bound states. This degeneracy is lifted by intervalley scattering [see Fig. 2]. The secular equation for the on-site impurity reduces to that of a scalar impurity with the replacement $V_{0,1} \to 4V_{0,1}$. Thus, additional intervalley scattering results also in a renormalization of the effective impurity strength. Note, however, that although both valleys K and K' are nontrivially coupled by the superconducting pairing and despite the pseudo spin nature of the valley degree of freedom, only real magnetic impurities act as pair breakers—a consequence of the Anderson theorem.[14]

IV. REAL-SPACE SIGNATURES OF THE IMPURITY STATES

With the real-space Green's function $G(x,x',\omega) = G^0(x - x',\omega) + G^0(x,\omega)T(\omega)G^0(-x',\omega)$ one obtains the local density of states $N(x,\omega) = N_0(\omega) + \delta N(x,\omega) = -\frac{1}{\pi}\mathrm{Im}\, G(x,x,\omega)$ in the presence of an impurity. This LDOS is a matrix corresponding to the matrix structure of the Green's function. It accounts for the contributions from the different sublattices, valleys, and the Nambu space. According to Eq. (1), the spin-up excitations are hole excitations yielding for each spin component the LDOS $N_{\downarrow\uparrow}(x,\omega) = \mathrm{Tr}\frac{\Lambda_0 \pm \Lambda_3}{2} N(x, \pm\omega)$, where the trace involves either the spin-down or -up part of the Nambu space. In the case of the scalar impurity, this yields the following corrections to the unperturbed LDOS in the continuum

$$\delta N_{\downarrow\uparrow}(r, \pm\omega) = -\frac{4}{\pi}\mathrm{Im}\frac{a_{\downarrow\uparrow} g_0^2(r,\omega) + b_{\downarrow\uparrow} g_1^2(r,\omega)}{1 - 2M(\omega)\omega V_1 + M^2(\omega)(\omega^2 - \Delta^2)(V_1^2 - V_0^2)}, \tag{5}$$

with $a_{\downarrow\uparrow} = (\omega^2 - \Delta^2)[\pm V_0 + M(\omega)\omega(V_0^2 - V_1^2)] + (\omega^2 + \Delta^2)V_1$ and $b_{\downarrow\uparrow} = (\pm V_0 + V_1) + M(\omega)\omega(V_0^2 - V_1^2)$.

By replacing $M(\omega) \to 4M(\omega)$ in these formulas, one obtains the case of the strongly localized on-site impurity. In STM experiments, graphene's lattice structure will give rise to a triangular modulation of the impurity states. This is neglected here, as similar effects in normal-state graphene have been discussed in Ref. 8.

Due to Eq. (5), the asymptotic decay of the intragap bound states at large distances from the impurity is governed by $g_0^2(r,\omega_0)$ and $g_1^2(r,\omega_0)$. Neglecting high-energy cut-off related oscillations at this length scale, one may extend the momentum space integrals in Eq. (2) to infinity. This yields modified Bessel functions, i.e., $g_0(r,\omega_0) = -\frac{1}{W^2}\mathrm{K}(0, r\sqrt{\Delta^2 - \omega_0^2}/v_f)$ and $g_1(r,\omega_0) = -\frac{i\sqrt{\Delta^2 - \omega_0^2}}{W^2}\mathrm{K}(1, r\sqrt{\Delta^2 - \omega_0^2}/v_f)$. Therefore, the wave functions of the impurity states decay as

$$\delta N_{\downarrow\uparrow}(r, \pm\omega_0) \propto r^{-1} e^{-2r\sqrt{\Delta^2 - \omega_0^2}/v_f}. \tag{6}$$

As Fig. 3 (left) shows, impurity states in the gap give rise to prominent features in future STM experiments: The density of the impurity state at the impurity site at $r = 0$ as well as the maximum of the density are strongly sensitive to the particular type of impurity. In general, impurity states with energies in the middle of the gap [$V_1 = 5$ W in Fig. 3 (left)] give rise to the sharpest maxima in the r-dependent LDOS. The ratio of the maximum density to the density at the impurity site increases with the potential strength V_1.

The ring structure corresponding to these impurity states in STM images may give a powerful experimental tool for identifying particular impurities present in superconducting graphene. This is in contrast to the normal-state graphene, where weak impurities do not give rise to resonances near the Dirac point and will therefore be hardly apparent in scanning tunneling spectroscopy (STS).[8]

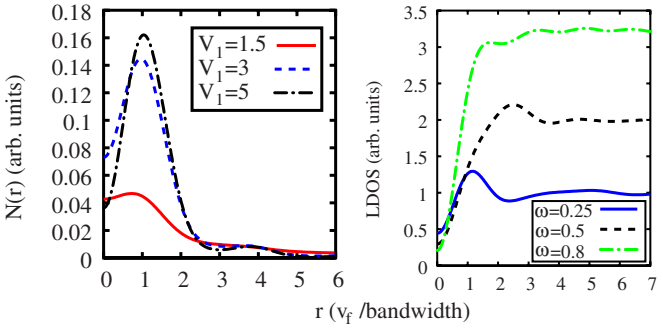

FIG. 3. (Color online) Left panel: Density N of the intragap bound states as a function of the distance r from the impurity for purely magnetic scalar impurities and different potentials V_1. The impurity strength is given in units of the bandwidth W. Right panel: Friedel oscillations in the LDOS around a scalar impurity at $r=0$ with $V_0=0$ and $V_1=3$ W. The different curves correspond to the energies $\omega=0.8$, 0.5 and 0.25 W. In both panels, the gap-parameter is $\Delta=W/10$.

In the continuum, Eq. (5) encodes the real-space shape of VBS and Friedel oscillations around the impurities. As Fig. 3 (right) shows exemplarily for a scalar impurity, the wavelength λ of these oscillations is always determined by the energy ω and the gap Δ: $\lambda=\pi v_f/\sqrt{\omega^2-\Delta^2}$. Besides these oscillations giving rise to standing-wave patterns in future STM experiments,[18] certain resonances due to VBS will be an even more prominent as well as impurity specific feature in these experiments: The LDOS in Fig. 3 (right) exhibits a characteristic peak at $r\approx 1$ and $\omega\approx 0.25$ W.

Apart from effects on the r-dependent LDOS at different energies corresponding to STM images at fixed bias, the impurities will manifest themselves also in the energy dependence of the LDOS at fixed position, which is accessible by STS. In Fig. 4, the LDOS near a purely magnetic scalar impurity with $V_0=0$ and $V_1=3$ W is compared to an impurity contributing an electrostatic potential $V_0=2$ W and $V_1=1$ W. The purely magnetic impurity, Fig. 4 (left), does not break particle-hole symmetry and yields therefore a fully symmetric LDOS and a fully antisymmetric local spin density of states (LSDOS). This is in contrast to the more general second impurity, Fig. 4 (right), where the LDOS and LSDOS are not symmetric under particle-hole transformation. Therefore, the degree of symmetry of the local spectra allows to estimate whether the impurity potential is magnetic

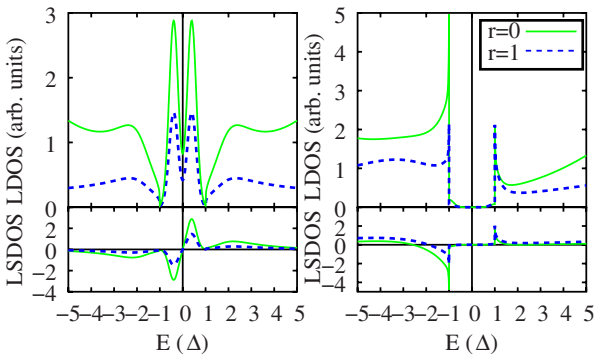

FIG. 4. (Color online) The LDOS (upper panel) and the LSDOS (lower panel), $\delta N_\uparrow(r,\omega)-\delta N_\downarrow(r,\omega)$, at $r=0$ and $r=1$ are shown for scalar of impurities with different potentials: a purely magnetic impurity with $V_0=0$ and $V_1=3$ W (left) as well as an impurity with $V_0=2$ W and $V_1=1$ W.

or not even in a non-spin-polarized STS experiment.

V. CONCLUSIONS

We argued that magnetic scattering will produce impurity induced bound and virtual bound states in superconducting graphene. These impurity states are similar to the Yu Lu-Shiba-Rusinov states in s-wave superconductors[9] and exhibit an intricate real-space and particle-hole dependent structure. Their spectroscopic and topographic properties predicted here are directly accessible by STM.[15,18] As each impurity generates a specific signature in the real-space LDOS, they provide a guideline for identifying the symmetry of the superconducting order parameter as well as different impurities in future experiments. Since the Cooper pairs have zero momentum we find the superconducting state in graphene to be a nontrivial example of valleytronics where valley quantum numbers are important.[12]

ACKNOWLEDGMENTS

The authors thank E. Andrei, C. Beenakker, A. H. Castro Neto, H. Fukuyama, A. Geim, P. J. Hirschfeld, M. I. Katsnelson, A. F. Morpurgo, I. Vekhter, and J. X. Zhu for useful discussions. This work was supported by U.S. DOE at Los Alamos and by Deutsche Forschungsgemeinschaft via SFB 668. T.O.W. is grateful to LANL and the T11 group for hospitality during the visit, when the ideas presented in this work were conceived.

*avb@lanl.gov, http://theory.lanl.gov

[1] K. S. Novoselov, A. K. Geim, S. V. Morozov, D. Jiang, Y. Zhang, S. V. Dubonos, I. V. Grigorieva, and A. A. Firsov, Science **306**, 666 (2004).

[2] K. S. Novoselov, A. K. Geim, S. V. Morozov, D. Jiang, M. I. Katsnelson, I. V. Grigorieva, S. V. Dubonos, and A. A. Firsov, Nature (London) **438**, 197 (2005).

[3] Y. Zhang, Y.-W. Tan, H. L. Stormer, and P. Kim, Nature (London) **438**, 201 (2005).

[4] C. Bena and S. A. Kivelson, Phys. Rev. B **72**, 125432 (2005).

[5] N. M. R. Peres, F. Guinea, and A. H. Castro Neto, Phys. Rev. B **73**, 125411 (2006).

[6] Y. V. Skrypnyk and V. M. Loktev, Phys. Rev. B **73**, 241402(R) (2006).

[7] V. V. Cheianov and V. I. Fal'ko, Phys. Rev. Lett. **97**, 226801 (2006).

[8] T. O. Wehling, A. V. Balatsky, M. I. Katsnelson, A. I. Lichtenstein, K. Scharnberg, and R. Wiesendanger, Phys. Rev. B **75**,

125425 (2007).
[9] A. V. Balatsky, I. Vekhter, and J.-X. Zhu, Rev. Mod. Phys. **78**, 373 (2006).
[10] V. M. Pereira, F. Guinea, J. M. B. Lopes dos Santos, N. M. R. Peres, and A. H. Castro Neto, Phys. Rev. Lett. **96**, 036801 (2006).
[11] H. B. Heersche, P. Jarillo-Herrero, J. B. Oostinga, L. M. K. Vandersypen, and A. F. Morpurgo, Nature (London) **446**, 56 (2007).
[12] A. Rycerz, J. Tworzydlo, and C. W. J. Beenakker, Nat. Phys. **3**, 172 (2007).
[13] M. Titov and C. W. J. Beenakker, Phys. Rev. B **74**, 041401(R) (2006).
[14] P. W. Anderson, J. Phys. Chem. Solids **11**, 26 (1959).
[15] A. Yazdani, B. A. Jones, C. P. Lutz, M. F. Crommie, and D. M. Eigler, Science **275**, 1767 (1997).
[16] C. Berger *et al.*, Science **312**, 1191 (2006).
[17] P. Mallet, F. Varchon, C. Naud, L. Magaud, C. Berger, and J. Y. Veuillen, Phys. Rev. B **76**, 041403(R) (2007).
[18] G. M. Rutter, J. N. Crain, N. P. Guisinger, T. Li, P. N. First, and J. A. Stroscio, Science **317**, 219 (2007).
[19] B. Uchoa and A. H. Castro Neto, Phys. Rev. Lett. **98**, 146801 (2007).
[20] The dielectric constant of graphene is $\epsilon \approx 6$ and implies good screening, see T. Ando, J. Phys. Soc. Jpn. **75**, 074716 (2006).
[21] C. W. J. Beenakker, Phys. Rev. Lett. **97**, 067007 (2006).